

Crystal Structure and Hirshfeld Surface Analysis of 1,4-Pentadien-3-one, (1*E*,4*E*)-1,5-diphenyl-2-(2,4-dinitrophenyl)hydrazone

Carolina B. P. Ligiéro,^a Pamella M. Monte,^a Tiago L. da Silva^b and José C. Barros^b*,^a

^aInstituto de Química, Universidade Federal do Rio de Janeiro, Av. Athos da Silveira Ramos, 149, CT, A-629, Cidade Universitária, 21941-909 Rio de Janeiro-RJ, Brazil

^bUniversidade Federal do Rio de Janeiro, Campus Macaé, Av. Aluizio da Silva Gomes, 50, 27930-560 Macaé-RJ, Brazil

The compound 1,4-pentadien-3-one,(1*E*,4*E*)-1,5-diphenyl-2-(2,4-dinitrophenyl)hydrazone presents the molecular formula C₂₃H₁₈N₄O₄ and was prepared in an undergraduate laboratory. The hydrazone was synthesized from the condensation between dibenzalacetone and 2,4-dinitrophenylhydrazine (DNPH) and crystallized employing water/acetone liquid-liquid diffusion. The structure presents three aromatic rings connected by an unsaturated Y-shaped system. Dinitro substituted and one of the other aromatic rings are 15° out of a coplanarity, while the other phenyl group is almost orthogonal to the first (89°). The only observed classical hydrogen bonding is an intramolecular N–H···O. The supramolecular structure was analyzed employing the Hirshfeld surface and that is organized through C–H···O hydrogen bond and C–H···π, polar-π, and π-stacking. An interaction involving NO₂···NO₂ was also observed.

Keywords: crystal structure, 2,4-dinitrophenylhydrazine, hydrazone

Introduction

Hydrazones are privileged structures in medicinal chemistry. They possess pharmacological activities like analgesic, anticonvulsant, antidepressant, anti-inflammatory and antiplatelet, antimalarial, antimicrobial, antimycobacterial, anti-Schistosomiasis, antitumoral, antiviral, and vasodilator.^{1,2} Hydrazone formation is a traditional identification and purification method (Brady's test)³ for aldehydes and ketones, thus we have prepared the compound 1,4-pentadien-3-one,(1*E*,4*E*)-1,5-diphenyl-2-(2,4-dinitrophenyl)hydrazone (**1**) as part of an undergraduate laboratory course by an established method employing accessible reagents.⁴ More recently, new applications of the hydrazone formation are the measurement of formaldehyde indoor or in cigarettes,^{5,6} removal of acrolein from active pharmaceutical ingredients (APIs)⁷ and finally the removal of aldehydes and ketones from essential oils by using a scavenger resin.⁸ The hydrazone (**1**) is easily synthesized, and crystallization provides large single crystals employing different methods and solvent systems. Such aspects raise this hydrazone as

an excellent example of crystallography teaching that can be extended to different aldehydes and ketones.

Experimental

Synthesis

Acetone, absolute ethanol, sulfuric acid PA (Vetec, Rio de Janeiro, Brazil) and 2,4-dinitrophenylhydrazine (Merck KGaA, Darmstadt, Germany) were used without further purification. Dibenzalacetone was prepared as described in the literature.⁴ The compound **1** (Scheme 1) was prepared from condensation between 2,4-dinitrophenylhydrazine (DNPH) and dibenzalacetone (1,5-diphenyl-1,4-pentadien-3-one): in an Erlenmeyer of 125 mL under magnetic stirring, 1.0 g of dibenzalacetone (4.3 mmol) was dissolved in absolute ethanol with gently heating (maximum of 60 °C). In another flask, 8.0 g of 2,4-DNPH were dissolved in 40 mL of H₂SO₄ and added to a mixture of 60 mL of water and 200 mL of ethanol. Then, 30 mL of the 2,4-DNPH acid solution was added into the dibenzalacetone mixture while stirring at room temperature for 15 min. After the time, the reaction mixture was filtered over a Buchner filter to obtain a red powder, then washed with cold

*e-mail: jbarros@iq.ufrj.br

Table 1. Crystallographic information

Crystal color/habit	red, prism
Crystal size / mm	0.45 × 0.07 × 0.04
Empirical formula	C ₂₃ H ₁₈ N ₄ O ₄
Formula weight / (g mol ⁻¹)	414.41
F(000)	864.0
Temperature / K	100
Absorption coefficient / mm ⁻¹	0.81
Calculated density / (g cm ⁻³)	1.393
Wavelength / Å	1.54180
<i>a</i> , <i>b</i> , <i>c</i> / Å	15.1306(10) 12.8166(9) 10.2338(7)
α , β , γ / degree	90.000 95.327(2) 90.000
Crystal system	monoclinic
Space group	<i>P</i> ₂ ₁ / <i>c</i>
Volume / Å ³	1976.0(2)
<i>Z</i> , <i>Z'</i>	4, 1
Diffractometer	Bruker D8 Venture APEX-III
Data collection	ϕ and ω scans on KAPPA goniometer
Reflections collected	26308
Independent reflections	3473
Absorption correction	multi-scan
<i>T</i> _{min} , <i>T</i> _{max}	0.611, 0.753
Theta range for data collection / degree	4.53 to 68.372
Index ranges	-18 < <i>h</i> < 18 -15 < <i>k</i> < 14 -12 < <i>l</i> < 12
Data/restraints/parameters	3473/0/284
Goodness-of-fit on <i>F</i> ²	1.06
Final residual factor [<i>I</i> > 2 σ (<i>I</i>)]	<i>R</i> ₁ : 0.0464 <i>wR</i> ₂ : 0.1270
Residual factor (all data)	<i>R</i> ₁ : 0.0490 <i>wR</i> ₂ : 0.1306
H-atom treatment	a mixture of independent and constrained refinement
Largest diff. peak and hole / (e Å ⁻³)	0.27, -0.25

a, *b*, *c*, α , β , γ : unit cell parameters; *Z*: formula unit per unit cell; *Z'*: formula unit per asymmetric unit; F(000): structure factor in the zeroth-order case; *F*: structure factor; *F*²: squared structure factor; *T*: transmission factor.

Table 2. Hydrogen bond geometry

D–H...A	Symmetry operation	D–H	H...A	D...A	D–H...A
N1–H1A...O1	–	0.89(2)	1.89(2)	2.6146(17)	127.4(18)
C5–H5...O2	1 – <i>x</i> , 1/2 + <i>y</i> , 3/2 – <i>z</i>	0.9500	2.5700	3.494(2)	166.00
C6–H6...O3	1 – <i>x</i> , 1/2 + <i>y</i> , 3/2 – <i>z</i>	0.9500	2.5200	3.4655(19)	170.00
C23–H23...O4	1 – <i>x</i> , 1/2 + <i>y</i> , 3/2 – <i>z</i>	0.9500	2.5500	3.451(2)	158.00

D, A: hydrogen bond donor and acceptor.

crystallization provided large single crystals employing different methods and solvent systems. The combination of synthesis and crystallization render this activity as an example of crystallography teaching, allows for improvement of the undergraduate curricula, and can be further extended to different aldehydes and ketones according to inventory availability.

The structure presents three aromatic rings, designated as A, B, and C (Figure 1b). A and B are almost orthogonal and their idealized least-square (LS) planes form an angle of 88.930(47)°. A and C are more coplanar and their ideal LS planes form an angle of 14.926(64)°. Dinitro substituted aromatic ring A is flat and exhibits the smallest HOMA (harmonic oscillator model of aromaticity) index (rms 0.0056, deviation from the idealized least-square planes; HOMA_A: 0.873).¹⁸ The orthogonal B is the most aromatic one (rms 0.0049; HOMA_B: 0.988), while the C ring presents slightly smaller local aromaticity when compared with B (rms 0.0053; HOMA_C: 0.976). Coplanar part of the unsaturated Y-like system (between A and C) exhibits slightly more equalized bonds than the orthogonal side, denoting better electronic conjugation between A and C.

Intramolecular hydrogen bonding leads to the formation of a six-membered planar ring (rms 0.0338) between hydrazone N–H and the *ortho* nitro group oxygen (Table 2).¹⁹ Hydrogen position (close to the nitrogen) was obtained from difference Fourier map (*F*_o – *F*_{calc}) and refined isotopically. Hydrogen bonding geometry is consistent with that described to other dinitrophenyl hydrazones like salicylaldehyde 2,4-dinitrophenylhydrazone (CCDC reference code BAFGUL01),²⁰ 4-(1-(2-(2,4-dinitrophenyl)hydrazino)butylidene)-5-methyl-2-phenyl-2,4-dihydro-3*H*-pyrazol-3-one *N,N*-dimethylformamide solvate (ZAKCAS),²¹ and (1*E*)-1-(3-bromophenyl)ethanone 2,4-dinitrophenylhydrazone (VABCUY).²² The structure of 2,4-DNPH (WASRAJ01) was redetermined in 2006.²³ A partially quinoidal structure for DNPH was suggested due to the low equalization of C–C aromatic bonds (HOMA calculated from data: 0.831), specially *ortho*-quinoidal. Here we observed some similar partial quinoidal behavior within A ring but is a less extend.

Hydrogen atoms of the dinitro-substituted A and nitro groups oxygens exhibit intermolecular self-assembly through C–H...O bonds giving rise to parallel linear polymeric tapes that grow along b axis (Figure 2). Distances in H...O contacts varies in the range 2.52–2.57 Å, shorter than the sum of van der Waals radii (2.72 Å).²⁴ Angles are in the range of 157–170°, indicating high directionality. They are organized by pairs of DD-AA interactions (D,A: hydrogen bond donator and acceptor) that give origin to rings with 11 (blue), 12 (orange), and 14 (yellow) members (Figure 2a). The overall graph set can be described as $C_4^4(6)[R_2^2(11), R_3^3(12), R_2^2(14)]$.¹⁹

C–H...O hydrogen bonds connect linearly each molecule to the other three. Fingerprint plot in Figure 3 demonstrates that H...O/O...H contacts are responsible for 24.2% of the Hirshfeld surface, with the formation of two sharp features and a broad blue area in the Hirshfeld surface.¹⁶ The polymeric tapes pile up with (201), but layering formation is prevented due to out of plane B-ring configuration, that establish CH... π and π - π interactions (Figure 2b). Intermolecular hydrogen bonds geometry data can be found in Table 2.

Nitro function presents a higher electronic density over both oxygens, which enable this group to act as Lewis base accepting hydrogen bonds. In Figure 4a the electrostatic potential was plotted over an electron density surface and the red-colored oxygens emerged surrounded by hydrogen atoms.¹⁶ This group, however, exhibit also a positive electrostatic portion described as a π -hole over the C–N bond.²⁵ This π -hole presents Lewis acid character and establishes an intermolecular interaction with oxygen from the nitro group, with N...O distance of 3.027 Å, slight smaller than the sum of the van der Waals radii (3.07 Å).²⁴ In the Figure 4a the complementary electrostatic character of the NO₂...NO₂ interaction is displayed. Each molecule of compound **1** is connected to the other two by the means

of nitro contacts, giving origin to a zig-zag chain motif observed along b axis in Figure 4b.

A polar- π almost parallel offset interaction was observed between A and B rings, with centroids separation of 3.9601(9) Å and the horizontal displacement of 2.127 Å; (the angle formed between the planes was 4.25°). Two of these supramolecular interactions are intermediated by one A...A parallel offset with centroids distance of 4.4809(9) Å, with horizontal displacement of the planes of 3.106 Å. Orthogonal B rings show a parallel offset π - π interaction toluene-like with centroids distance of 3.7985(10) Å (horizontal displacement of 1.598 Å). In the fingerprint plot,¹⁶ C...C interactions give origin to the light blue portion in the 1.8 vs. 1.8 π -stacking region (Figure 3). B ring π ... π contact is sandwiched between two C–H... π hydrogen bonds. These π interactions are summarized in Figure 5.

Despite exhibiting one basic nitrogen (from hydrazone group), the participation of N...H/H...N interactions are almost negligible in the supramolecular structure, probably because of steric effects.

The crystal packing view along b axis is displayed in Figure 6. It is possible to observe alternation between the A-ring hydrogen-bonded motif and B-ring with π interactions.

A search in the Cambridge Structural Database (CSD, version 5.41, 2020.0 CSD, last update November 2019) through the software CONQUEST with the keyword “hydrazone” returned 1661 hits.^{26,27} Delimiting the search to dinitrophenyl hydrazone, a total of 191 hits were found. Most of the structures exhibit both nitro groups and the aromatic ring in a flat (or near flat) configuration. In the vast majority of these crystal structures, an intramolecular hydrogen bond was observed between hydrazone N–H and oxygen from nitro at the *ortho* position. Notable exceptions were the derivatives of 6-chloro-2,4-dinitrophenylhydrazine,

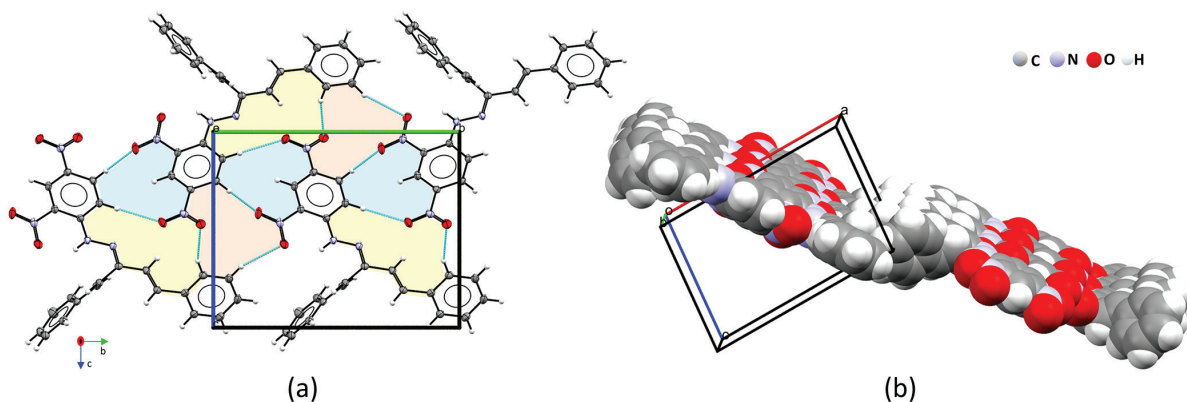


Figure 2. Polymeric linear motif formed by self-assembly of the aromatic cores; (a) thermal ellipsoids at 50% of probability, view down a axis; (b) space-filling model displaying C–H...O pattern.

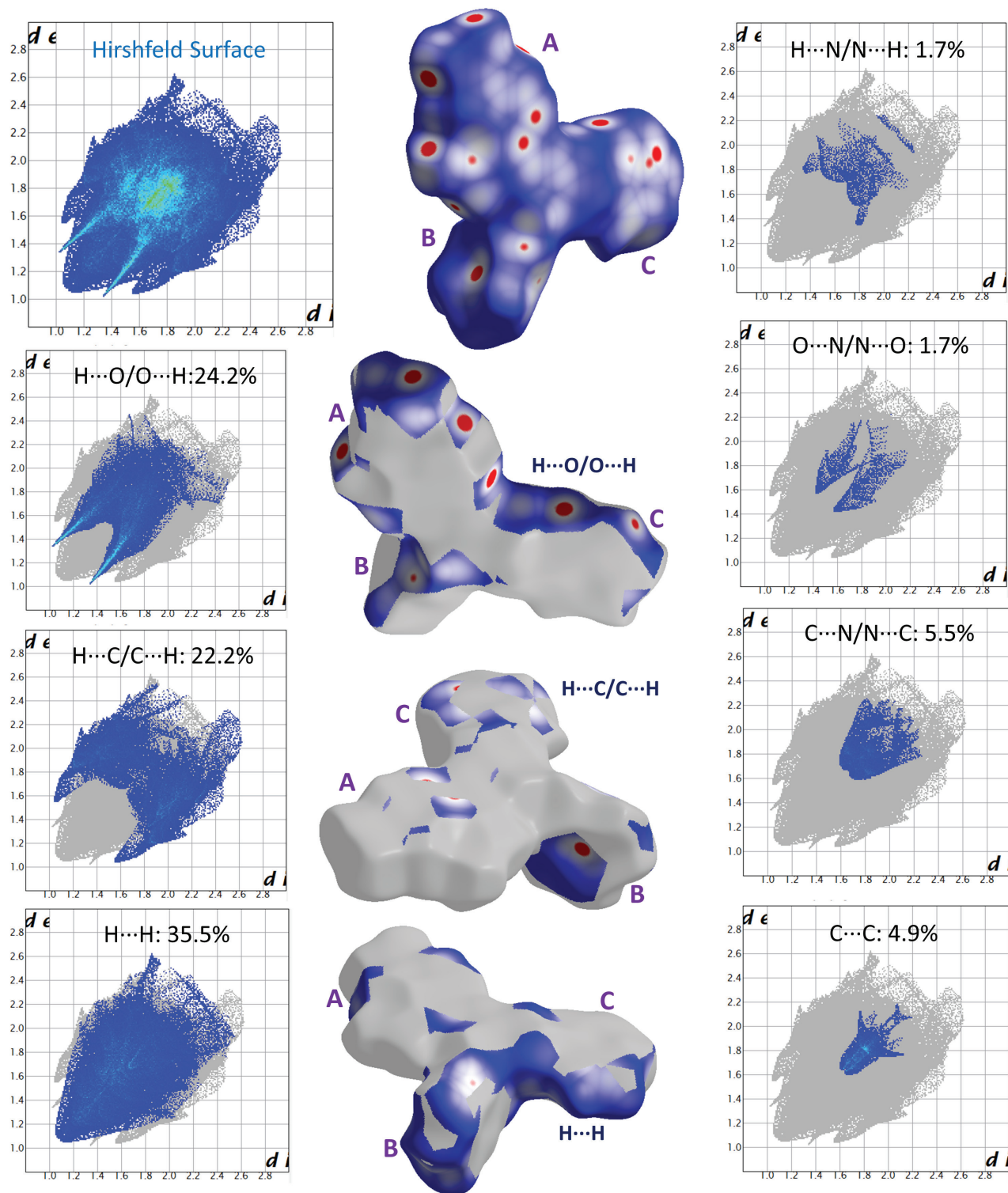


Figure 3. Hirshfeld surface isovalue 0.5 (d_{norm} from -0.1556 to 1.3875) and fingerprint plot d_i vs. d_e where: d_{norm} is the normalized contact distance in the Hirshfeld surface; d_i is the distance from the surface to the nearest nucleus internal to the surface; d_e is the distance from the surface to the nearest nucleus external to the surface. The red points indicate where the distance is smaller than the sum of the van der Waals radii.

an agent for the absolute structure determination.²⁸ Such hydrazones present both chlorine and nitro substituents in the *ortho* positions, but the *ortho* group adopts a different orientation, far from N–H and with about 60° of torsion.

Some examples are EDUJAO, EDUJES, EDUJOC, and GANQAO.²⁹

MOGUL²⁶ analysis revealed that most of the structural aspects of compound **1** find similarities with

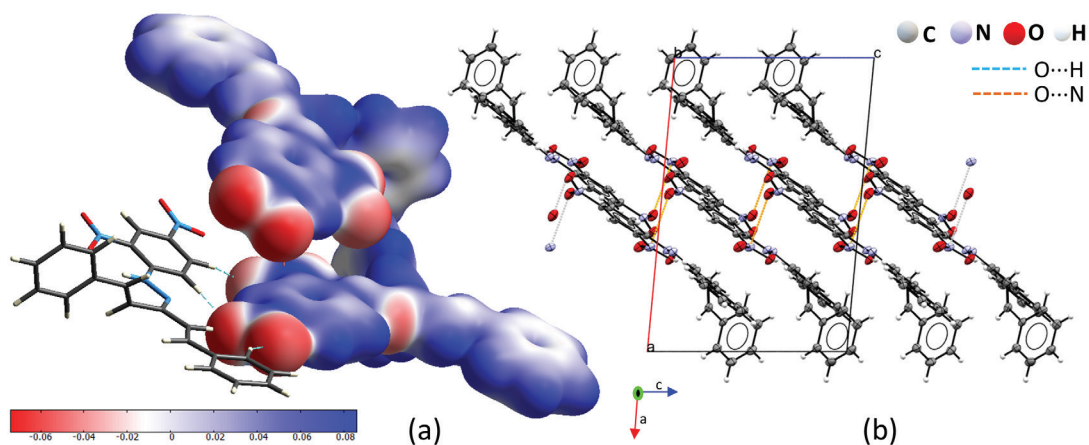


Figure 4. Nitro...nitro interaction: (a) electrostatic potential plotted over an electron density surface (B3LYP/6-31G(d,p); isovalue 0.008); (b) view down b face, N...O contacts highlighted, drawn with thermal ellipsoids at 50%.

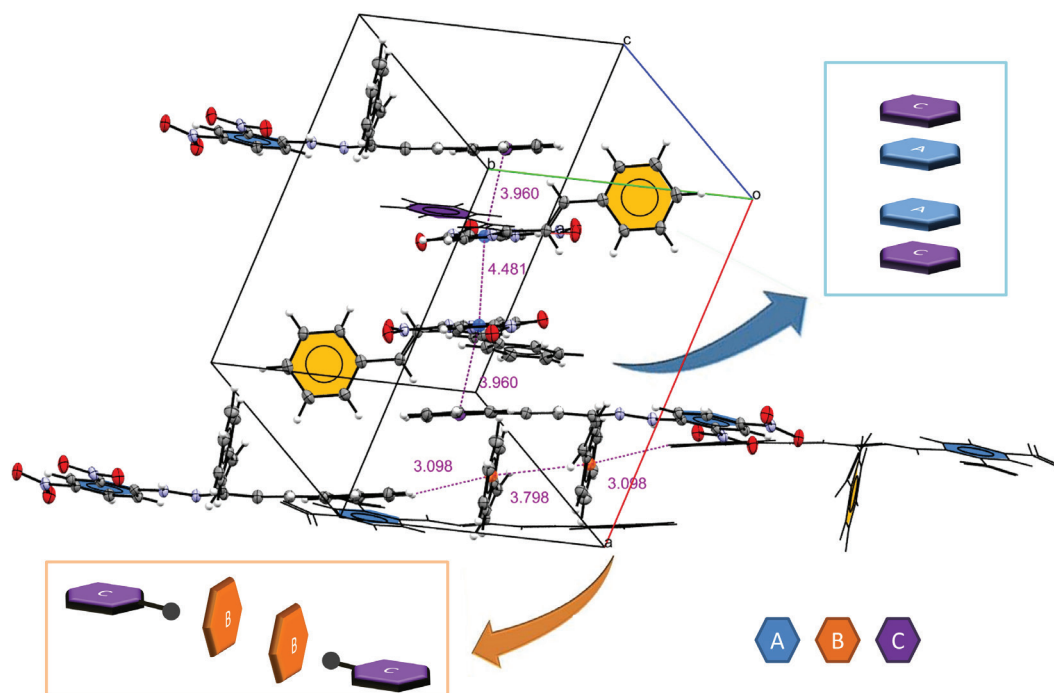


Figure 5. Intermolecular face-to-face and face-to-edge interactions.

related hydrazones. Some aspects concerned with C7 neighborhood, although are unusual: the angle formed by C7–N2–N1 fragment, of 116.17° (the average is 118.45° among 15 related hits). The torsion angle of 116.51° in the fragment C9–C8–C7–N2 is also unusual (common angle is closer to 180°). Such unusual aspects can be attributed to the presence of two phenylethene moieties bonded to C7.

Conclusions

A combination of synthesis and crystallization was employed to obtain single crystals of a hydrazone. The red

prisms obtained represents a crystallography demonstration to improve undergraduate curricula.

Supplementary Information

Crystallographic data (excluding structure factors) for the structures in this work were deposited in the Cambridge Crystallographic Data Centre as supplementary publication number CCDC 2009611. Copies of the data can be obtained, free of charge, via <https://www.ccdc.cam.ac.uk/structures/>.

Supplementary crystallographic data are available free of charge at <http://jbc.sbc.org.br> as PDF file.

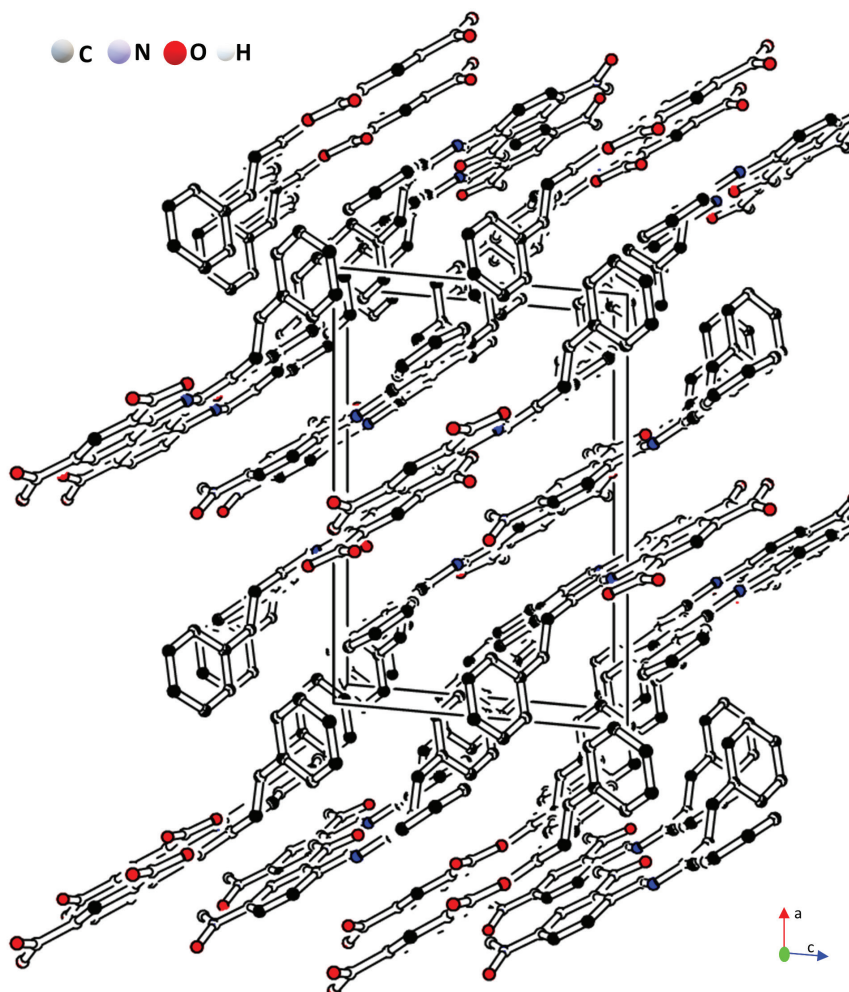


Figure 6. Crystal packing view along b axis; hydrogen atoms omitted for clarity.

Acknowledgments

We would like to acknowledge professor Pierre M. Esteves, Lygia de Moares and Ministério da Ciência, Tecnologia, Inovações e Comunicações (MCTIC), Financiadora de Estudos e Projetos (FINEP), LDRX (Laboratório Multiusuário de Difração de Raios-X da UFF), and Centro Nacional de Biologia Estrutural e Bioimagem (CENABIO) for the support with the X-ray diffraction facility (D8-Venture).

References

1. Rollas, S.; Küçükgülzel, G.; *Molecules* **2007**, *12*, 1910.
2. Verma, G.; Marella, A.; Shaquiquzzaman, M.; Akhtar, M.; Ali, M. R.; Alam, M. M.; *J. Pharm. Bioallied Sci.* **2014**, *6*, 69.
3. Brady, O. L.; Elsmie, G. V.; *Analyst* **1926**, *51*, 77.
4. Madureira, A. M.; Santana, A. B.; Valente, E.; U-Ferreira, M. J. In *Comprehensive Organic Chemistry Experiments for the Laboratory Classroom*; Afonso, C. A. A.; Candeias, N. R.; Simão, D. P.; Trindade, A. F.; Coelho, J. A. S.; Tan, B. R., eds.; The Royal Society of Chemistry: Cambridge, 2017, p. 272.
5. Gillett, R. W.; Kreibich, H.; Ayers, G. P.; *Environ. Sci. Technol.* **2000**, *34*, 2051.
6. Wong, J. W.; Ngim, K. K.; Eiserich, J. P.; Yeo, H. C. H.; Shibamoto, T.; Mabury, S. A.; *J. Chem. Educ.* **1997**, *74*, 1100.
7. Kecili, R.; Nivhede, D.; Billing, J.; Leeman, M.; Sellergren, B.; Yilmaz, E.; *Org. Process Res. Dev.* **2012**, *16*, 1225.
8. Mendonça, A. D. M.; Oliveira, A. V. B.; Cajaiba, J.; *Org. Process Res. Dev.* **2017**, *21*, 1794.
9. <https://www.compoundchem.com/2016/11/07/24-dnp/>, accessed in September 2020.
10. APEX3, version 2019.1-0; Bruker AXS Inc., Madison, Wisconsin, USA, 2016; SAINT, version 8.40A; Bruker AXS Inc., Madison, Wisconsin, USA, 2016; SADABS, version 2016/2; Bruker AXS Inc., Madison, Wisconsin, USA, 2016.
11. Sheldrick, G. M.; *Acta Crystallogr., Sect. A: Found. Adv.* **2008**, *A64*, 112.

12. Farrugia, L. J.; *J. Appl. Crystallogr.* **2012**, *45*, 849.
13. Sheldrick, G. M.; *Acta Crystallogr., Sect. C: Struct. Chem.* **2015**, *C71*, 3.
14. Spek, A. L.; *Acta Crystallogr., Sect. D: Struct. Biol.* **2009**, *D65*, 148.
15. Macrae, C. F.; Edgington, P. R.; McCabe, P.; Pidcock, E.; Shields, G. P.; Taylor, R.; Towler, M.; van de Streek, J.; *J. Appl. Crystallogr.* **2006**, *39*, 453.
16. McKinnon, J. J.; Jayatilaka, D.; Spackman, M. A.; *Chem. Commun.* **2007**, 3814.
17. Spackman, M. A.; McKinnon, J. J.; Jayatilaka, D.; *CrystEngComm.* **2008**, *10*, 337.
18. Krygowski, T. M.; Cyrański, M. K.; *Chem. Rev.* **2001**, *101*, 1382.
19. Etter, M. C.; *J. Phys. Chem.* **1991**, *95*, 4601.
20. Monfared, H. H.; Pournalimardan, O.; Janiak, C.; *Z. Naturforsch* **2007**, *62b*, 717.
21. Idemudia, O. G.; Holsten, E. C.; *Crystals* **2016**, *6*, 127.
22. Jasinski, J. P.; Guild, C. J.; Chidan Kumar, C. S.; Yathirajan, H. S.; Mayekar, A. N.; *Acta Crystallogr., Sect. E: Crystallogr. Commun.* **2010**, *E66*, o2832.
23. Wardell, J. L.; Low, J. N.; Glidewell, C.; *Acta Crystallogr., Sect. C: Struct. Chem.* **2006**, *C62*, 318.
24. Bondi, A.; *J. Phys. Chem.* **1964**, *3*, 441.
25. Baúza, A.; Sharko, A. V.; Senchyk, G. A.; Rusanov, E. B.; Frontera, A.; Domasevitch, K. V.; *CrystEngComm.* **2017**, *19*, 1933.
26. Bruno, I. J.; Cole, J. C.; Edgington, P. R.; Kessler, M.; Macrae, C. F.; McCabe, P.; Pearson, J.; Taylor, R.; *Acta Crystallogr., Sect. B: Struct. Sci., Cryst. Eng. Mater.* **2002**, *B58*, 389.
27. Bruno, I. J.; Cole, J. C.; Kessler, M.; Luo, J.; Motherwell, W. D. S.; Purkis, L. H.; Smith, B. R.; Taylor, R.; Cooper, R. I.; Harris, S. E.; Orpen, A. G.; *J. Chem. Inf. Comput. Sci.* **2004**, *44*, 2133.
28. Kawai, Y.; Hayashi, M.; Tokitoh, N.; *Tetrahedron Lett.* **2002**, *43*, 465.
29. Kawai, Y.; Hayashi, M.; Tokitoh, N.; *Tetrahedron* **2005**, *61*, 5049.

Submitted: June 13, 2020

Published online: September 30, 2020

